Published in final edited form as:
J Org Chem. 2012 June 1; 77(11): 4939–4948. doi:10.1021/jo300314z.

A Theoretical Study of Cyclohexyne Addition to Carbonyl-C_α Bonds: Allowed and Forbidden Electrocyclic and Non-Pericyclic Ring Openings of Strained Cyclobutenes

C. Avery Sader and **K. N. Houk***
Department of Chemistry and Biochemistry, University of California, Los Angeles, California 90095-1569

Abstract

The mechanism of cyclohexyne insertion into a C(O)-C_α bond of cyclic ketones, explored experimentally by the Carreira group, has been investigated using density functional theory. B3LYP and M06-2X calculations were performed in both gas phase and THF (CPCM, UAKS radii). The reaction proceeds through a stepwise [2+2] cycloaddition of cyclohexyne to the enolate, followed by three disparate ring opening possibilities of the cyclobutene alkoxide to give the product: 1) thermally-allowed conrotatory electrocyclic ring opening, 2) thermally-forbidden disrotatory electrocyclic ring opening, or 3) non-pericyclic C-C bond cleavage. Our computational results for the model alkoxide and potassium alkoxide systems show that the thermally-allowed electrocyclic ring opening pathway is favored by less than 1 kcal/mol. In more complex systems containing a potassium alkoxide (**e**–**f**), the barrier of the allowed conrotatory ring opening is disfavored by 4–8 kcal/mol. This suggests that the thermodynamically more stable disrotatory product can be formed directly through a "forbidden" pathway. Analysis of geometrical parameters and atomic charges throughout the ring opening pathways provides evidence for a non-pericyclic C-C bond cleavage, rather than a thermally-forbidden disrotatory ring opening. A true forbidden disrotatory ring opening transition structure was computed for the cyclobutene alcohol; however, it was 19 kcal/mol higher in energy than the allowed conrotatory transition structure. An alternate mechanism in which the disrotatory product forms via isomerization of the conrotatory product was also explored for the alkoxide and potassium alkoxide systems.

Introduction

Arynes and cycloalkynes are potentially useful building blocks in organic synthesis.[1–3] Stoltz and Tambar have reported a mild direct aryne insertion into C-C bonds.[1] They obtained an unexpected C-C addition product (boxed; Scheme 1) in comparable yield with the expected product.

Carreira and co-workers recently reported the formal addition of cyclohexyne to C-C bonds of cyclic ketones to yield medium-sized fused ring systems.[2] This process involves simultaneous formation of an enolate from a cyclic ketone and formation of cyclohexyne via base-induced elimination from an iodonium salt of cyclohexene. In some cases, a tricyclic product containing a cyclobutene ring is produced, suggesting the intermediacy of this [2+2] cycloaddition product in formation of the cycloheptenone, as shown in Scheme 2.

*Corresponding Author: houk@chem.ucla.edu.

Supporting Information
Cartesian coordinates, computed total energies of all optimized structures, imaginary frequencies of all transition structures, and plots of ChelpG atomic charges. This material is available free of charge via the Internet at http://pubs.acs.org.

Carreira and Gampe have applied this reaction to the total synthesis of guanacastepenes,[3] and a comprehensive review of their applications of this ring expansion reaction has recently been documented.[4] Comandini and Brezinsky computationally explored the potential energy surface of a radical/π-bond addition mechanism of *o*-benzyne to cyclopentadiene. One of the multiple pathways they studied involved the disrotatory electrocyclic ring opening of a strained cyclobutene; however, it seems that the allowed conrotatory ring opening was not considered.[5] To determine the details of this cycloalkyne insertion mechanism a computational study using density functional theory (DFT) calculations was initiated. Of prime interest in this study was the nature of the electrocyclic ring opening step.

Computational Methods

Intermediate and transition state geometry optimizations were performed with Gaussian 09 using the hybrid functional B3LYP with the 6-31G(d) basis set or LANL2DZ for potassium.[6] In addition, the anions were optimized with the diffuse 6-311++G(d,p) basis set. A stability check of the restricted wavefunction was performed to insure that open-shell wavefunctions are not more stable.[7] Analytical frequencies were calculated for each optimized structure using the corresponding level of theory. Single point energy calculations were performed with M06-2X/6-311++G(d,p) on B3LYP/6-31G(d) geometries and thermally corrected using the B3LYP/6-31G(d) vibrational data in order to report enthalpies. Such calculations have been shown to give improved thermodynamics for C-C bond forming reactions.[8] All optimized saddle points were explored by Intrinsic Reaction Coordinate (IRC)[9,10] calculations, ensuring that they connect the appropriate reactants and products on the potential energy surface.

The effects of THF solvation on the reaction energetics were evaluated using the conductor-like polarizable continuum solvation model (CPCM).[11] The solute surface was defined by UAKS radii.[12]

Results and Discussion

1. Reaction of cyclohexyne and cyclopentanone enolate

The cycloaddition step was confirmed by our calculations to be stepwise, in accordance with the Woodward-Hoffmann rules. The energetics of cycloaddition are summarized in Figure 1.

Nucleophilic attack on cyclohexyne is the first step of the reaction and occurs without an activation barrier. Examples of nucleophilic additions to cycloalkynes without a barrier of activation have been reported elsewhere in the literature.[13] The addition is exceedingly exothermic, forming **3a** with a ΔH of −36 to −48 kcal/mol. Our calculations show that the alkyne (**1**) is distorted from linearity by 48°, which is in agreement with past theoretical studies of cyclohexyne using Hartree-Fock, DFT, or Møller-Plesset perturbation theory methods.[14–16] The C-C and C-O bond lengths in cyclopentanone enolate (**2a**) are representative of enolate character. Figure 2 shows the geometries of cyclopentanone enolate nucleophilic addition to cyclohexyne optimized in the gas phase with B3LYP/6-31G(d) and B3LYP/6-311++G(d,p).

Ring closure of vinyl anion **3a** to form cyclobutene alkoxide **5a** has an activation barrier of only 2–5 kcal/mol and is exothermic by only 6–7 kcal/mol. Structural deviations from normal cyclobutene geometries are immediately apparent in the bond lengths of **5a**. A computational study by Houk and Rondan showed that donor substituents like alkoxide groups interact strongly with the C_3–C_4 σ* orbital in cyclobutene, thereby lowering the barrier to ring opening.[17] This hyperconjugative effect results in an increase of the C_3–C_4 bond length as well as a decrease of the C_3-O bond length relative to unsubstituted

cyclobutene and is evident in the C_3–C_4 bond length of 1.69 Å and the C_3-O bond length of 1.31 Å.

Electrocyclic ring opening of **5a** is the next step in the pathway, and the energetics are summarized in Figure 3. The experimental enthalpy of activation for the electrocyclic ring opening of cyclobutene is 32.5 ± 0.5 kcal/mol, and the reaction is exothermic by 10.8 kcal/mol.[18] According to the Woodward-Hoffmann rules, cyclobutene undergoes a symmetry-allowed conrotatory ring opening under thermal conditions. Numerous experimental and computational studies have confirmed this preference.[17–21] Specifically, experiments by Brauman and Golden estimated that the allowed conrotatory process is 15.0 kcal/mol more favorable than the forbidden disrotatory process.[21] The results of our computational study showed the enthalpy of activation for the allowed conrotatory electrocyclic ring opening of **5a** is 4.8 (6.0) kcal/mol, and the reaction is exothermic by 8.0 kcal/mol by B3LYP, but slightly endothermic by M06-2X. Non-pericyclic C-C bond cleavage gave an enthalpy of activation of 5.5 (8.0) kcal/mol and an exothermicity of 34 kcal/mol, only slightly higher than the allowed conrotatory pathway. We use the term “non-pericyclic” since there appears to be no cyclic delocalization, and this transition state appears to be different from pseudopericyclic transition states of electrocyclization reactions. The term “pseudopericyclic” was first used by Lemal to describe reactions that are characterized by the exchange of roles between orthogonal bonding and nonbonding atomic orbitals.[22] Computational investigations have provided evidence that psuedopericyclic transition states are typically planar with no rotation of the terminal π-bonds. For instructive reviews of the subject, the reader is directed to articles of Kappe et al.,[23] Birney et al.,[24] and references therein. Isomerization of **7a** via **8a** forms the more stable product **7a′**. The difference between the enthalpies of reaction in the conrotatory and non-pericyclic cases is due to formation of a strained *cis*, *trans*-cycloheptadiene skeleton in the former and a relatively stable *cis*, *cis*-cycloheptadiene skeleton in the latter.

The optimized geometries of conrotatory and non-pericyclic ring opening are shown in Figure 4. Previous work has shown that the skeleton of the conrotatory transition structure of cyclobutene is nonplanar (φ≈15°), while the disrotatory transition structure is planar.[25] It was also found that constraining planarity in the conrotatory transition structure reduces overlap between the σ orbital of the breaking bond and the π orbital present in cyclobutene. It was concluded that this reduction in stabilizing orbital overlap lowers the preference for the allowed conrotatory pathway. As seen in Figure 4, the $C_3C_2C_1C_4$ dihedral angle of the conrotatory transition structure is 5°, considerably more planar than the transition state of cyclobutene itself.

A number of investigations in the literature provide evidence that *cis-trans* isomerization can occur in similarly strained systems, directly connecting conrotatory products to disrotatory products on the potential energy surface.[26–29] No such transition structure was found using spin-restricted B3LYP; however, use of broken symmetry, spin-unrestricted B3LYP successfully yielded structure **8a** (Figure 5). This result clearly indicates diradical character, which is known to exist in transition structures of π-bond rotation. Elongated C_1–C_4 and C_2–C_3 bond lengths relative to **6a** indicate more single- bond character and provide further evidence for the diradical nature of **8a**. The decreased C_1–C_2 bond length also supports this idea. It is worthwhile to note that the C_3–C_4 distance has increased almost to its final value of 3.20 Å as seen in **7a′**, while a comparatively small amount of outward rotation of C_4-H has occurred. The enthalpy of activation for *cis-trans* isomerization was calculated as 12 kcal/mol.

2. Reaction of cyclohexyne and cyclopentanone potassium enolate in THF

An equivalent analysis of the reaction mechanism and energetics was performed with cyclohexyne and cyclopentanone potassium enolate. While potassium will be solvated in solution, this model provides a picture of the extreme effect of ion pairing on the reaction pathway. The energetics of cycloaddition are summarized in Figure 6. The addition yields an intermediate with a ΔH of −40 kcal/mol. For ring closure, an activation barrier of 3 kcal/mol was computed and the reaction is exothermic by 8 kcal/mol.

Figure 7 shows the geometries of cyclohexyne insertion into cyclopentanone potassium enolate optimized in THF with B3LYP/6-31G(d), using LANL2DZ for potassium. As shown by the bond distances in **3b** and **4b**, the potassium ion is stabilizing the development of charge on both the oxygen of the cyclopentanone enolate and C2 of cyclohexyne. A C_3–C_4 bond length of 1.64 Å and a C_3-O bond length of 1.35 Å in **5b** both indicate less donation of electron density of oxygen into the σ* orbital of C_3–C_4 when compared to the bare enolate. As a direct consequence, the barrier to electrocyclic ring opening of **5b** is 10 kcal/mol greater than the electrocyclic ring opening of **5a** (Figures 3 and 8).

The electrocyclic ring opening step favors the allowed conrotatory process by about 1 kcal/mol; however, unlike the case of cyclopentanone enolate, the barrier of *cis-trans* isomerization is greater than both the barrier for subsequent ring closing (reversion) and the barrier for non-pericyclic ring opening. The energetics of ring opening are summarized in Figure 8. Optimized geometries of conrotatory and non-pericyclic ring opening are shown in Figure 9. The $C_3C_2C_1C_4$ dihedral angles of the conrotatory and non-pericyclic transition structures are 18° and −4°, respectively, which closely resemble 19° and ~0°,[25] those of the ring opening transition structures of cyclobutene itself. There is an apparent interaction between the potassium and C4 in the non-pericyclic transition structure (**6b′**), but the preference for the allowed conrotatory ring opening is less than 1 kcal/mol, about the same as in the free alkoxide. The reaction leading to the conrotatory product **7b** is endothermic by 8 kcal/mol. As in the case where potassium is absent, the large thermodynamic difference between **7b** and **7b′** is due to the presence of a trans double bond in the 7-membered conrotatory product.

A transition structure connecting the *cis/trans* product **7b** to the *cis/cis* product **7b′** is shown in Figure 10. Like the free alkoxide, *cis-trans* isomerization by direct π-bond rotation occurs here, necessitating the use of open-shell DFT to locate this transition structure. The C_3–C_4 bond elongates from 1.38 Å to 1.50 Å, and the C_2–C_3 bond elongates from 1.42 Å to 1.46 Å. The C_3–C_4 bond length of 3.15 Å and $C_3C_2C_1C_4$ dihedral angle of −4° in **8b** are both essentially the final values observed in **7b′**. Interestingly, the C_4C_3O bond angle has increased to 175°, more than that seen in the disrotatory product, while the C_3C_4H bond angle has only increased by 10° relative to **7b**. The activation enthalpy of *cis-trans* isomerization was calculated as 14 kcal/mol.

A better model for the experimental reaction conditions would be a fully THF-solvated potassium enolate, but this would be computationally highly challenging. The results are expected to be somewhere between the results for the potassium-coordinated and free anions.

3. Ring opening of the cyclobutene alcohol

We have also explored the extreme of coordination to the cyclobutene alkoxide, namely the corresponding alcohol. These results provide an assessment of allowed vs. forbidden processes on a more conventionally substituted cyclobutene. Stationary points on the energy surface of electrocyclic ring opening computed with B3LYP/6-31G(d) are shown in Figure

11. Thermally corrected M06-2X/B3LYP-6311++G(d,p) single point energies on B3LYP/6-31G(d) geometries are shown in parentheses. There is a preference of 19–21 kcal/mol for the allowed conrotatory ring opening of the cyclobutenol, in spite of the 30 kcal/mol energetic preference for the less strained product that would result from forbidden disrotatory opening. This indicates that the normal preference for the allowed pathway is operating, in spite of large thermodynamic differences in the reactions.

The optimized geometries of conrotatory and disrotatory ring opening of cyclobutenol are shown in Figure 12. The C_3–C_4 bond length of 1.60 Å in **5c** is unusually long, but less stretched than the corresponding alkoxide. The bond angles and dihedral angles in the ring opening transition structures are not appreciably different from those in the previous cases, but the three C-C bond lengths in the ring are nearly identical, showing significant delocalization that was not observed in the other cases. Conrotatory electrocyclic ring opening is endothermic by 17–18 kcal/mol, while disrotatory ring opening is exothermic by 12–14 kcal/mol. A summary of computed enthalpies for the model reaction including all basis sets and solvent models used is shown in Table 1. An analogous table reporting Gibbs free energies is given in the Supporting Information (Table S1).

4. Ring opening of an alkoxide-substituted guanacastepene precursor

Next, we expanded the investigation of ring opening energetics to more complex systems incorporated by Carreira.[3] The electrocyclic ring opening of anion **5d** was shown to favor the allowed conrotatory process; however, the observed preference of less than 1 kcal/mol is essentially negligible when considering error in B3LYP/6-31G(d) calculations. The thermally corrected M06-2X/6-311++G(d,p)//B3LYP/6-31G(d) single point energies show the energy gap to be 2 kcal/mol. Conrotatory product **7d** is less stable than cyclobutene enolate **5d** by 1 kcal/mol, while disrotatory product **7d′** is more stable than **5d** by 32 kcal/mol. The energetics of ring opening are shown in Figure 13.

Optimized geometries of conrotatory and non-pericyclic ring opening are shown in Figure 14. The C_3C_4 bond length in **5d** is 1.68 Å, shorter than the 1.73 Å distance seen in the B3LYP/6-31G(d) optimized structure of cyclobutene enolate **5a**. This difference can be attributed to a decrease in donation of the C_3-O nonbonding orbital into the C_3C_4 σ* orbital due to electrostatic interactions of the alkoxide with hydrogens on an adjacent ring (**5d**, Figure 14), an effect qualitatively similar to coordination of the alkoxide with K^+. This interaction is observed throughout the process of ring opening. The C_3C_4 distances are very similar in the two transition structures **6d** and **6d′**, 2.39 Å and 2.43 Å respectively, unlike those seen when comparing the allowed and forbidden transition structures **6a–c** and **6a′–c′**. The $C_3C_2C_1C_4$ dihedral angles of **6d** and **6d′** are −17° and 13° respectively. As mentioned previously, the disrotatory ring opening transition structure of cyclobutene is planar,[25] so an observed dihedral angle of 13° in **6d′** is indicative of non-pericyclic character. Interestingly, the positive dihedral angles in **6d′** become negative in **7d′**. As a result, the carbon adjacent to C4 in the cycloheptadiene ring has flipped from the concave to the convex side of the molecule.

5. Ring opening of a potassium alkoxide-substituted guanacastepene precursor

The thermally allowed conrotatory electrocyclic ring opening of potassium alkoxide **5e** was disfavored by 8 kcal/mol, in sharp contrast to all other systems studied. Conrotatory product **7e** is less stable than **5e** by 9 kcal/mol, while **7e′** is more stable than **5e** by 22 kcal/mol. Stationary points detailing the energetics of ring opening of **5e** are presented in Figure 16.

Optimized geometries of conrotatory and non-pericyclic ring opening are shown in Figure 17. The transition structure of isomerization from **7e** to **7e′** is shown in Figure 18. All

relevant geometrical information is presented with the same interpretations as provided before; however, there is one important difference. In this molecule, there are other oxygen atoms to which the potassium atom can coordinate. Specifically in **6e′**, the coordination of the potassium to C4 and to another oxygen is likely responsible for the stabilization of this transition structure relative to **6e**. With that idea in mind, a slight modification was made to replace the two oxygens in the adjacent ring with methylene carbons to form **5f**. Ring opening structures are shown in Figure 19, while Table 2 summarizes the ring opening energies of **5d–f**. Although replacing the oxygens in the ring with methylene groups did lower the energy difference between **6f** and **6f′** relative to **6e** and **6e′**, Table 2 indicates a preference of 4 kcal/mol still remains for non-pericyclic ring opening over conrotatory electrocyclic ring opening. See Table S2 in the Supporting Information for Gibbs free energies.

6. ChelpG calculations on the mechanism of ring opening

ChelpG (charges from electrostatic potentials using a grid based method)[28] calculations on B3LYP/6-31G(d) optimized geometries were used to characterize the electronic structure of all ring opening systems. Unlike the conrotatory transition structure of cyclobutene, the conrotatory transition structures **6a**–**f** possess unequal charge distribution throughout the ring due to electronic effects originating from the oxygen on C3. The magnitude of negative charge on the oxygens in the non-pericyclic transition structures is close to that in the intermediates. This is uncharacteristic of electronic structure changes in pericyclic reactions, in which atomic charges gradually change throughout ring opening. C4 develops a full negative charge in the anionic systems, decreasing from −0.1 in alkoxide **5** to −1.1 in transition state **6′**. In the potassium alkoxide systems, this charge buildup on C4 is stabilized by coordination of the potassium cation. Together, the trends in electronic structure of oxygen and C4 through **5**–**6′**–**7′** provide evidence against a pericyclic disrotatory ring opening. Instead, the mechanism resembles carbonyl formation in the transition state with anion migration to C4 upon C-C bond cleavage (Scheme 4). Ring opening of **5c** is the only system that displays true forbidden disrotatory nature, as shown by the magnitude of difference in energies between the two pathways and the plots of atomic charges. Figure 20 shows the atomic charges of the four carbons in the cyclobutene ring and of the oxygen on C3 throughout both ring opening pathways of **5a**. Corresponding plots of all systems presented in this paper and numerical tables of charges are given in the Supporting Information.

Conclusions

The large preference for allowed conrotatory ring opening in the cyclobutene alcohol becomes very small in the alkoxide, presumably due to the very early transition states arising from the very large exothermicity of the reaction. The C_1–C_4 and C_2–C_3 bonds in **6a**, **6a′**, **6b**, and **6b′** show primarily single bond character (1.46–1.52 Å), which, along with the fact that the C_1–C_2 bonds are 1.34–1.36 Å, indicates a very early transition state.

In the gas phase reaction of the free alkoxide, the mechanism is a conrotatory electrocyclic ring opening pathway that is preferred by 1–3 kcal/mol, followed by *cis-trans* isomerization with a barrier of 6–12 kcal/mol to give the experimentally observed product (Figure 3). In the reaction model where oxygen is coordinated with potassium in THF, as seen in Figure 8, conrotatory ring opening is also preferred by about 1 kcal/mol; however, *cis-trans* isomerization is unfeasible at low temperatures as this barrier is 7 kcal/mol higher than the barrier for electrocyclic ring closing. This suggests a mechanism in which there is equilibration of conrotatory ring opening and closing with a percentage of non-pericyclic ring opening to give the thermodynamic product. In the gas phase reaction of the free

alkoxide **5d**, the mechanism is an allowed conrotatory ring opening followed by *cis-trans* isomerization to give **7d′**. For the ring openings of potassium alkoxides **5e** and **5f** in THF, the mechanism follows a non-pericyclic ring opening that is 8 kcal/mol and 4 kcal/mol lower than conrotatory ring opening, respectively. This appears to be the mechanism studied by the Carreira group. ChelpG calculations of the ring opening pathways help show that the forbidden “disrotatory” mechanism is, in fact, non-pericyclic in nature.

Supplementary Material

Refer to Web version on PubMed Central for supplementary material.

Acknowledgments

We are grateful to the National Institutes of Health for financial support (R01 GM036700), and to Erick M. Carreira for helpful discussions.

References

1. Tambar UK, Stoltz BM. J Am Chem Soc. 2005; 127:5340–5341. [PubMed: 15826170]
2. Gampe CM, Boulos S, Carreira EM. Angew Chem Int Ed. 2010; 49:4092–4095.
3. Gampe CM, Carreira EM. Angew Chem Int Ed. 2011; 50:2962–2965.
4. Gampe CM, Carreira EM. Angew Chem Int Ed. 2012; 51:3766–3778.
5. Comandini A, Brezinsky K. J Phys Chem A. 2012; 116:1183–1190. [PubMed: 22214520]
6. Frisch, MJ., et al. Gaussian 09, revision A.02. Gaussian, Inc; Wallingford, CT: 2009.
7. Staroverov VN, Davidson ER. J Am Chem Soc. 2000; 122:7377–7385.
8. Pieniazek SN, Clemente FR, Houk KN. Angew Chem, Int Ed. 2008; 47:7746–7749.
9. Fukui K. J Phys Chem. 1970; 74:4161–4163.
10. Deng L, Ziegler T. Int J Quantum Chem. 1994; 52:731–765.
11. Barone V, Cossi M. J Phys Chem A. 1998; 102:1995–2001.
12. Takano Y, Houk KN. J Chem Theory Comput. 2005; 1:70–77.
13. Cheong PHY, Paton RS, Bronner SM, Im GYJ, Garg NK, Houk KN. J Am Chem Soc. 2010; 132:1267–1269. [PubMed: 20058924]
14. Olivella S, Pericàs MA, Riera A, Solé A. J Org Chem. 1987; 52:4160–4163.
15. Johnson RP, Daoust KJ. J Am Chem Soc. 1995; 117:362–367.
16. Yavari I, Nasiri F, Djahaniani H, Jabbari A. Int J Quantum Chem. 2005; 106:697–703.
17. Rondan NG, Houk KN. J Am Chem Soc. 1985; 107:2111–2121.
18. Cooper W, Walters WD. J Am Chem Soc. 1958; 80:4220–4224.
19. Dolbier WR Jr, Koroniak H, Houk KN, Sheu C. Acc Chem Res. 1996; 29:471–477.
20. Breulet J, Schaefer HF III. J Am Chem Soc. 1984; 106:1221–1226.
21. Brauman JI, Golden DM. J Am Chem Soc. 1968; 90:1920–1921.
22. Ross JA, Seiders RP, Lemal DM. J Am Chem Soc. 1976; 98:4325–4327.
23. Fabian WMF, Bakulev VA, Kappe CO. J Org Chem. 1998; 63:5801–5805. [PubMed: 11672180]
24. Ji H, Li L, Xu X, Ham S, Hammad LA, Birney DM. J Am Chem Soc. 2009; 131:528–537. [PubMed: 19140791]
25. Lee PS, Sakai S, Hörstermann P, Roth WR, Kallel EA, Houk KN. J Am Chem Soc. 2003; 125:5839–5848. [PubMed: 12733925]
26. López CS, Faza ON, de Lera AR. Chem Eur J. 2007; 13:5009–5017. [PubMed: 17372999]
27. Qin C, Davis SR. J Org Chem. 2003; 68:9081–9087. [PubMed: 14604384]
28. Johnson RP, Daoust KJ. J Am Chem Soc. 1996; 118:7381–7385.
29. Inoue Y, Hagiwara S, Daino Y, Hakushi T. J Chem Soc Chem Commun. 1985; 19:1307–1309.
30. Breneman CM, Wiberg KB. J Comput Chem. 1990; 11:361–373.

31. Guner V, Khuong KS, Leach AG, Lee PS, Bartberger MD, Houk KN. J Phys Chem A. 2003; 107:11445–11459.
32. Houk KN. Acc Chem Res. 1975; 8:361–369.
33. Woodward RB, Hoffmann R. Angew Chem Int Ed. 1969; 8:781–853.
34. Evans DA, Golob AM. J Am Chem Soc. 1975; 97:4765–4766.

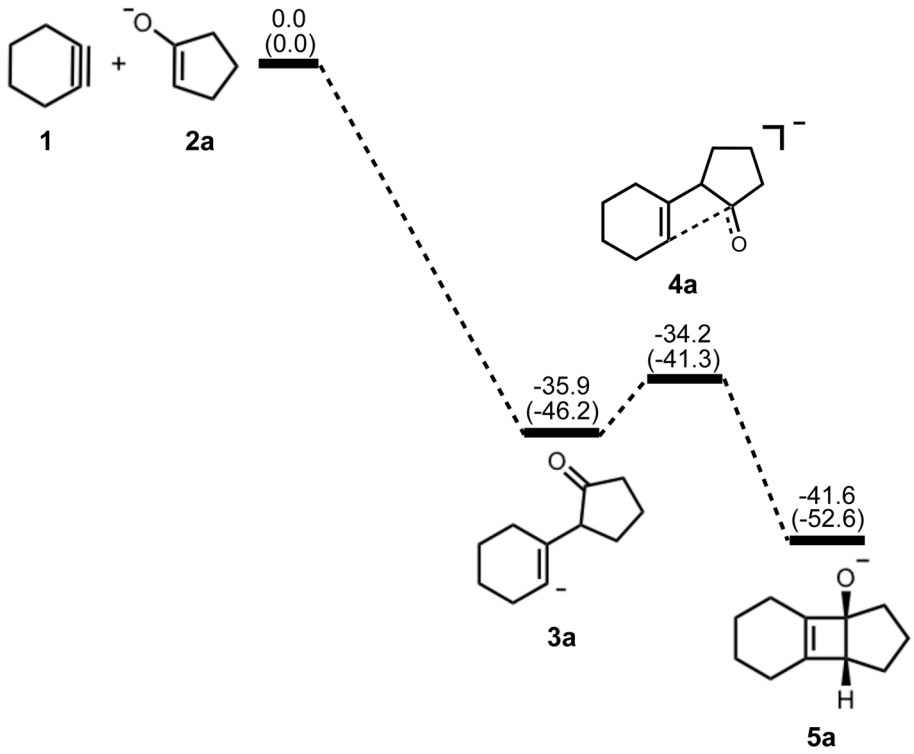

Figure 1.
Stationary points on the energy surface for cycloaddition of cyclohexyne and cyclopentanone enolate. B3LYP/6-311++G(d,p) thermal energies, *ΔH*, with thermally corrected M06-2X/6-311++G(d,p)//B3LYP/6-31G(d) energies, ΔH, in parentheses, shown in kcal/mol.

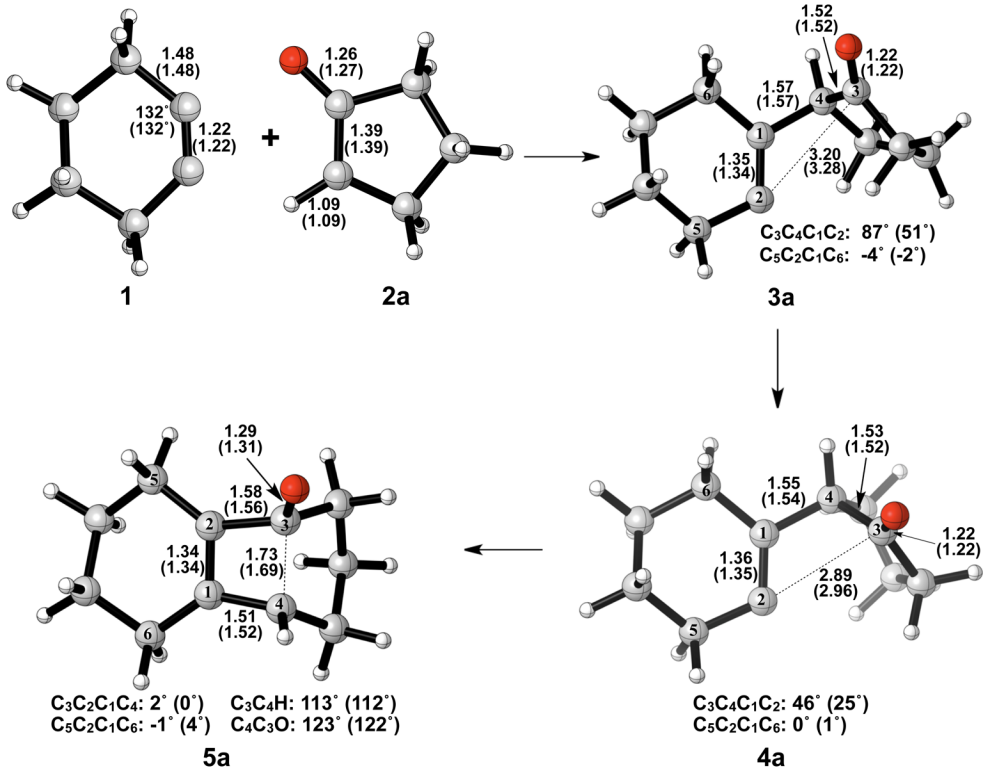

Figure 2.

Optimized geometries of cyclohexyne insertion into cyclopentanone enolate. B3LYP/6-31G(d) selected bond distances (Å), angles, and dihedral angles with B3LYP/6-311++G(d,p) in parentheses, are shown.

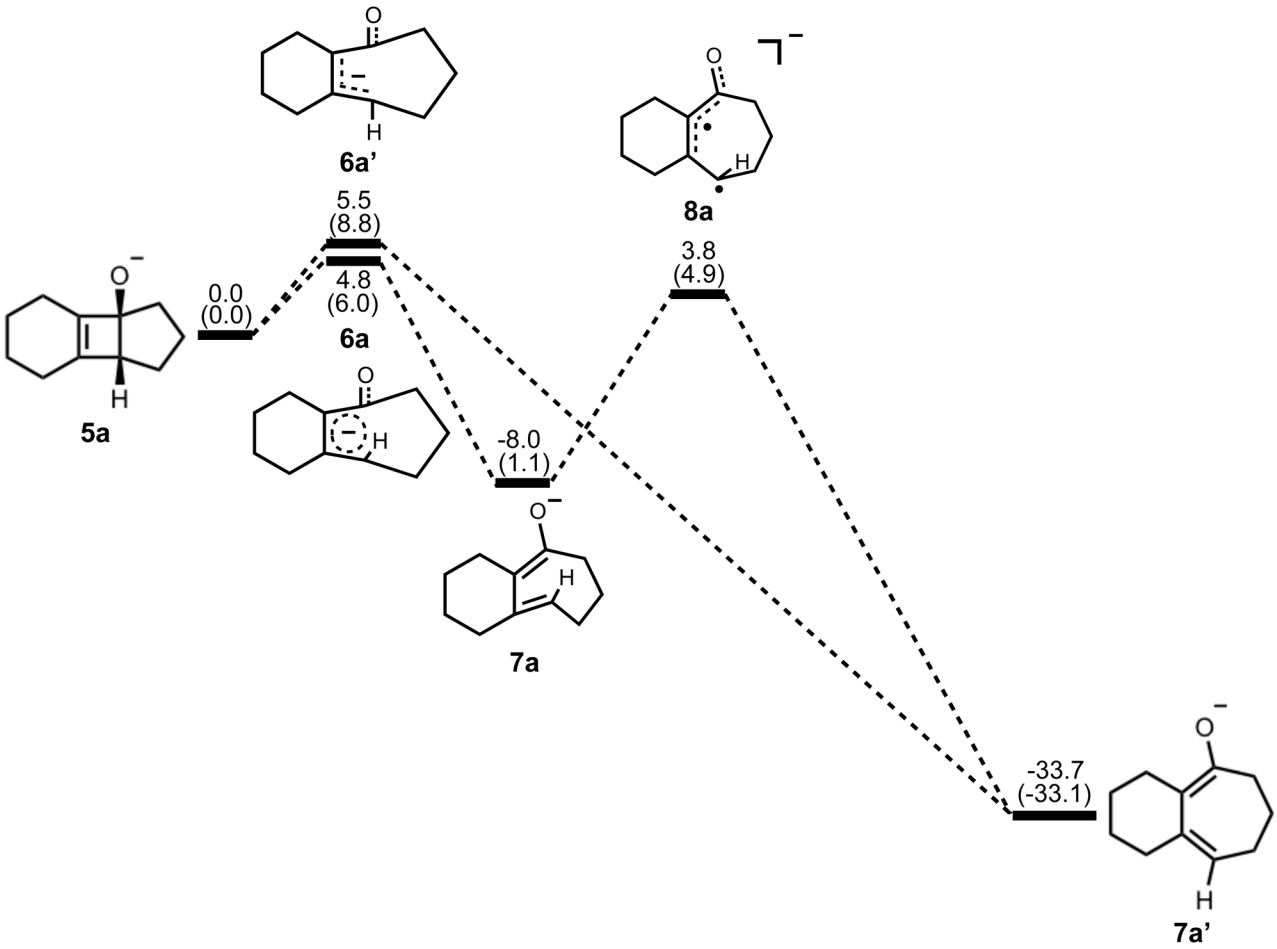

Figure 3.
Stationary points on the energy surface for electrocyclic ring opening and *cis-trans* isomerization. B3LYP/6-311++G(d,p) thermal energies, ΔH, with thermally corrected M06-2X/6-311++G(d,p)//B3LYP/6-31G(d) energies, ΔH, in parentheses, shown in kcal/mol.

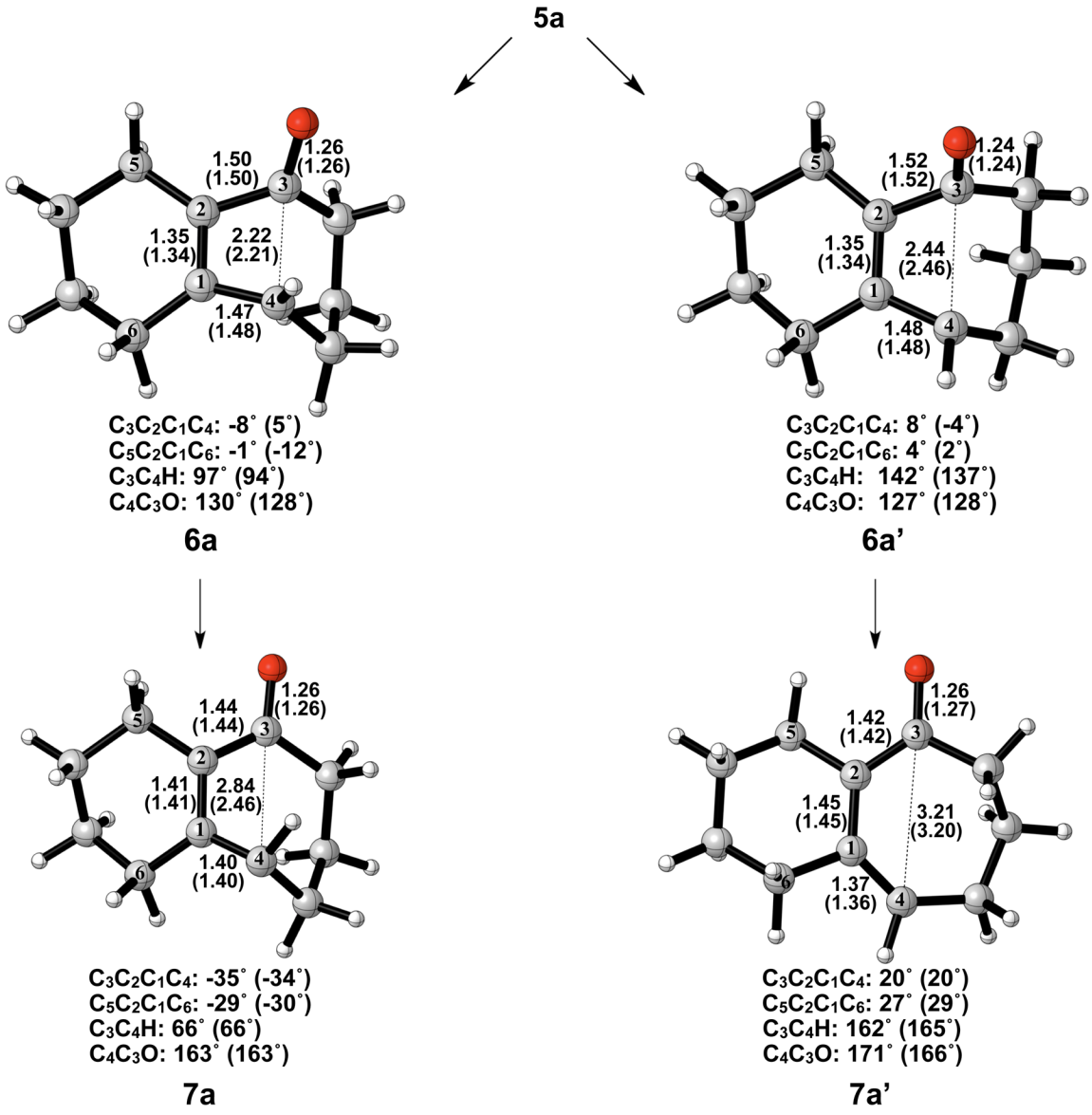

Figure 4.

Optimized geometries of conrotatory (left) and non-pericyclic (right) ring opening of cyclobutene alkoxide **5a**. B3LYP/6-31G(d) selected bond distances (Å) and dihedral angles, with B3LYP/6-311++G(d,p) in parentheses, are shown.

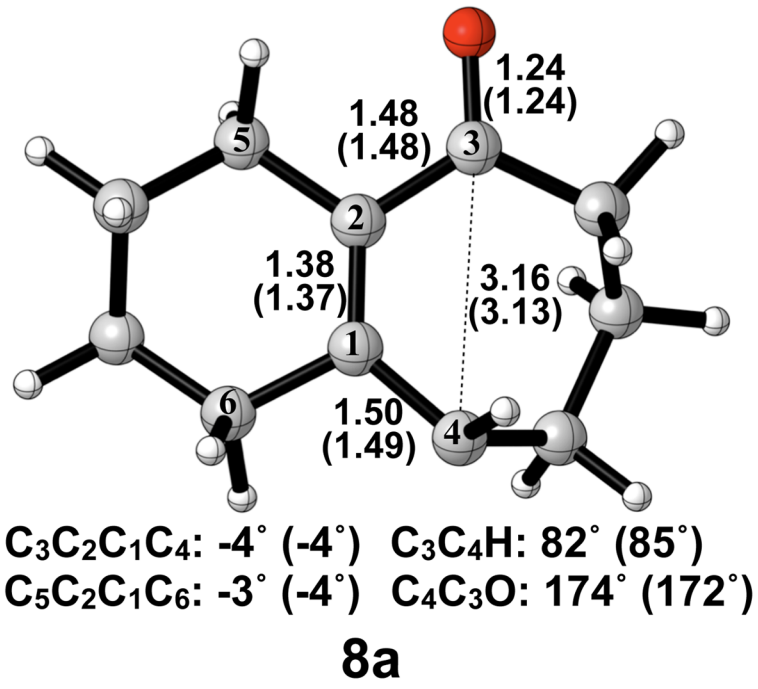

Figure 5.
Optimized transition structure of *cis-trans* isomerization of alkoxide intermediate **7a** to **7a′**. B3LYP/6-31G(d) selected bond distances (Å), angles, and dihedral angles, with B3LYP/6-311++G(d,p) in parentheses, are shown.

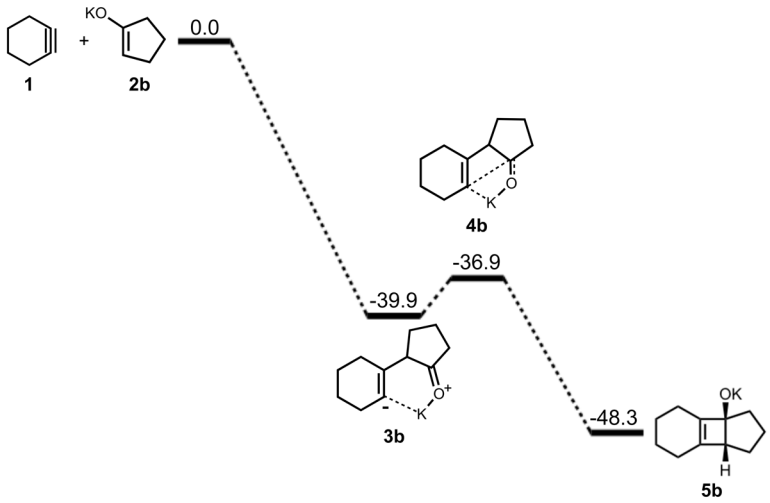

Figure 6.
Stationary points on the energy surface for cycloaddition of cyclohexyne and cyclopentanone potassium enolate. B3LYP/6-31G(d) thermal energies, ΔH, shown in kcal/mol.

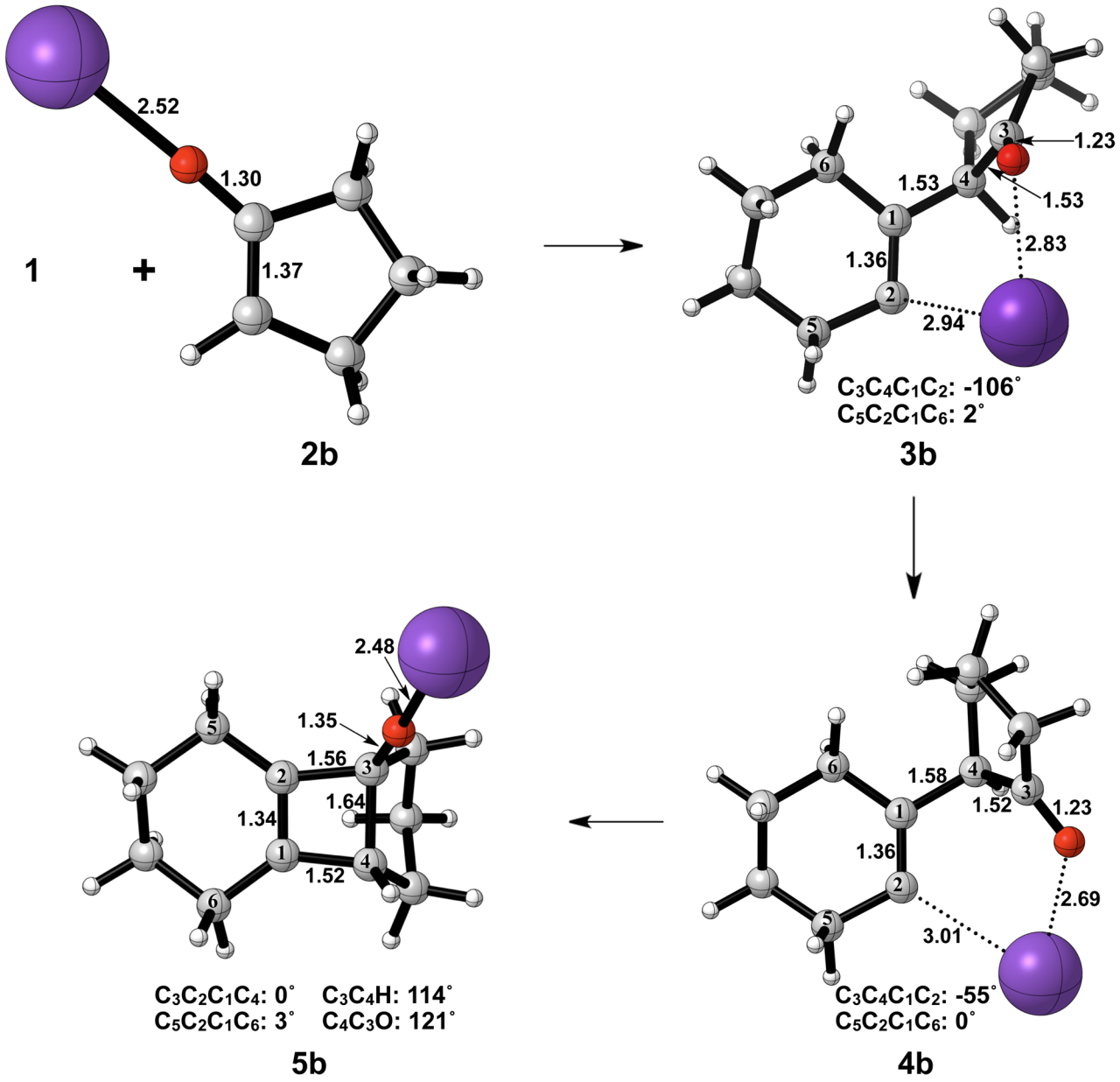

Figure 7.
Optimized geometries in the cyclohexyne insertion into cyclopentanone potassium enolate. B3LYP/6-31G(d) selected bond distances (Å), angles, and dihedral angles are shown. LANL2DZ was used for potassium.

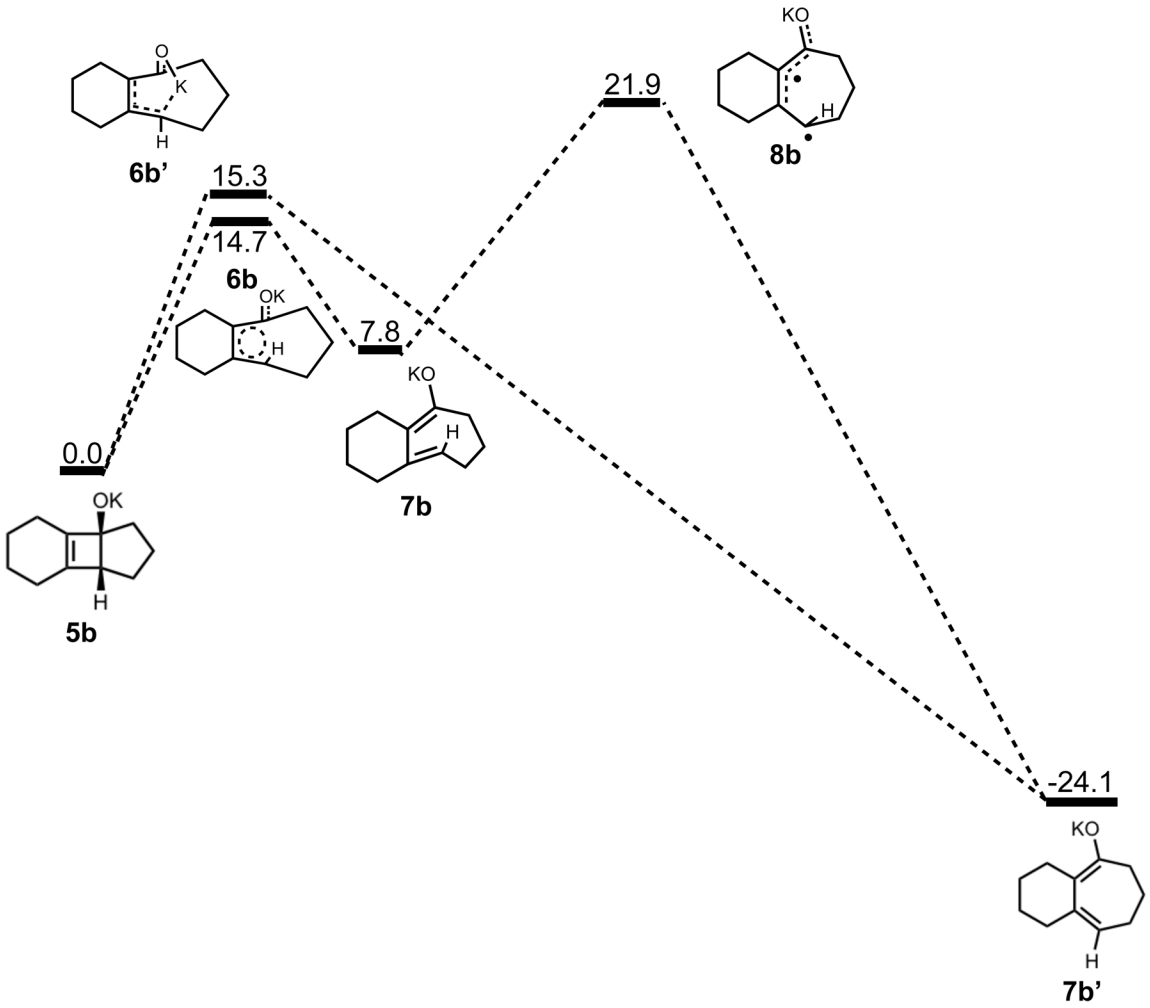

Figure 8.
Stationary points on the energy surface for electrocyclic ring opening and *cis-trans* isomerization. B3LYP/6-31G(d) thermal energies, ΔH, shown in kcal/mol.

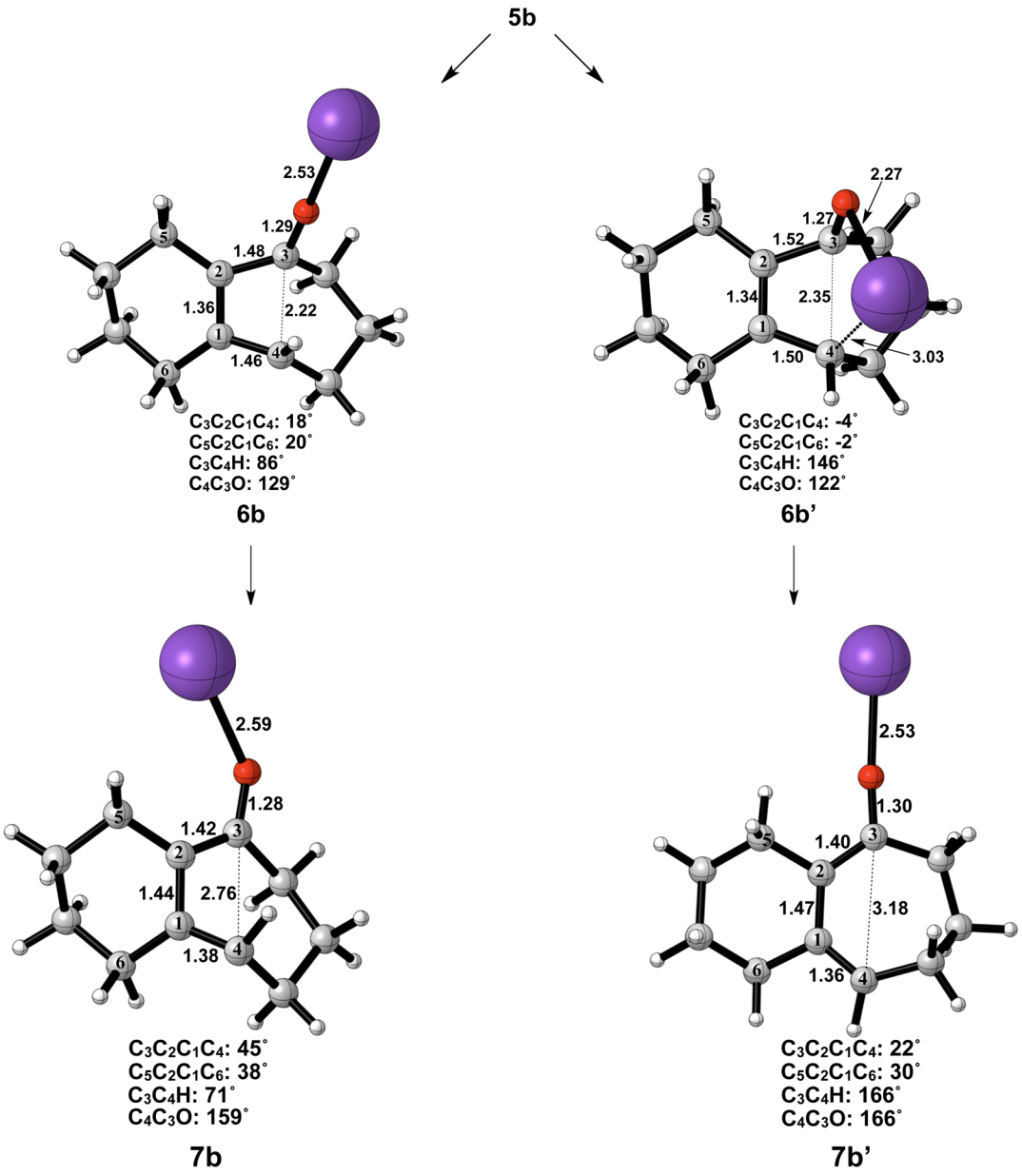

Figure 9.

Optimized geometries of conrotatory (left) and non-pericyclic (right) ring opening of cyclobutene potassium alkoxide **5b**. B3LYP/6-31G(d) selected bond distances (Å), angles, and dihedral angles are shown. LANL2DZ was used for potassium.

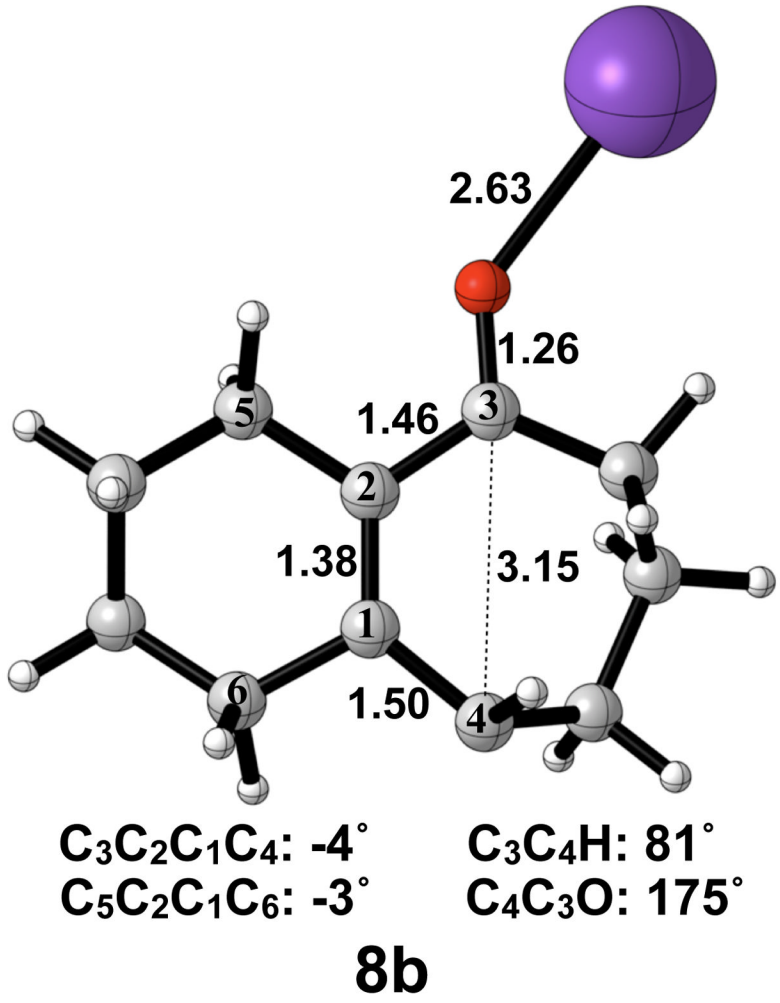

Figure 10.
Optimized transition structure of isomerization of potassium alkoxide intermediate **7b** to **7b**′. B3LYP/6-31G(d) selected bond distances (Å), angles, and dihedral angles are shown.

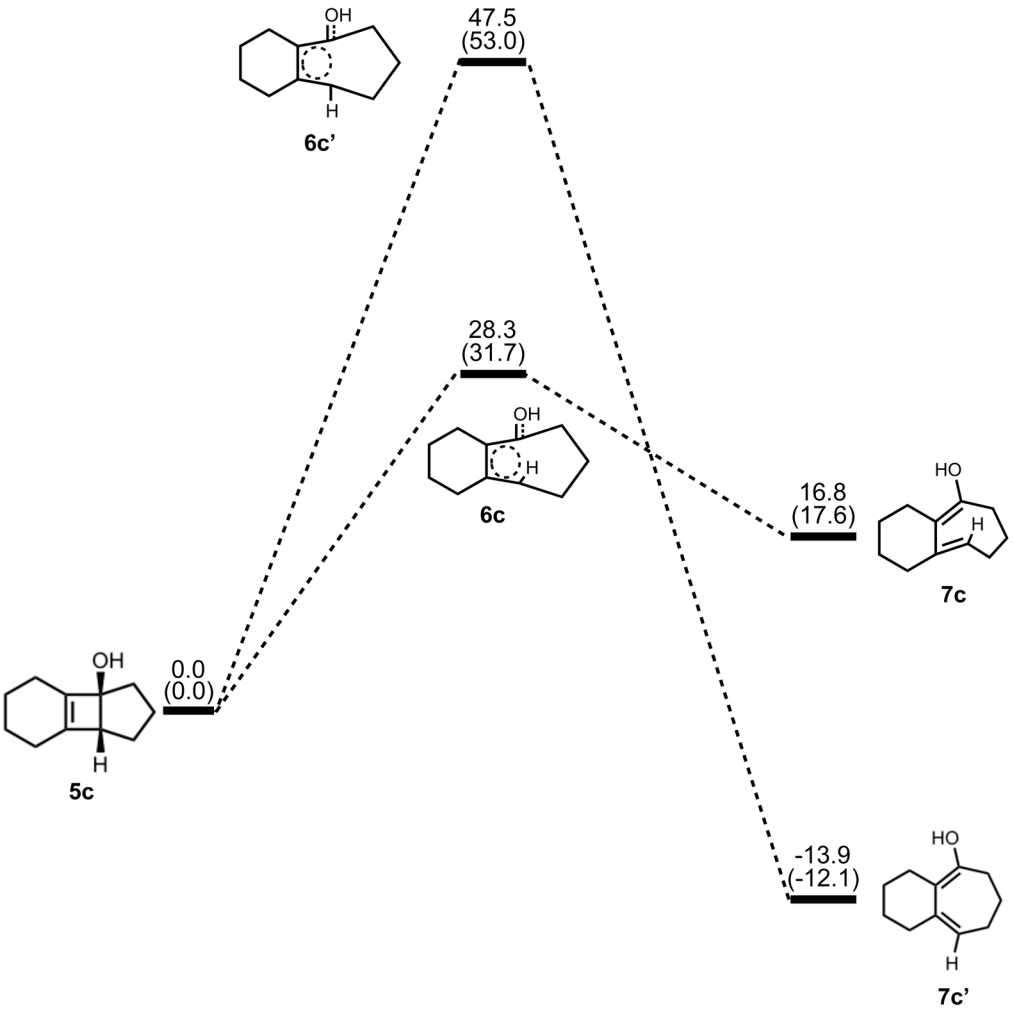

Figure 11.

Stationary points on the energy surface for electrocyclic ring opening. B3LYP/6-31G(d) thermal energies, ΔH, with thermally corrected M06-2X/6-311++G(d,p)//B3LYP/6-31G(d) energies, ΔH, in parentheses, shown in kcal/mol.

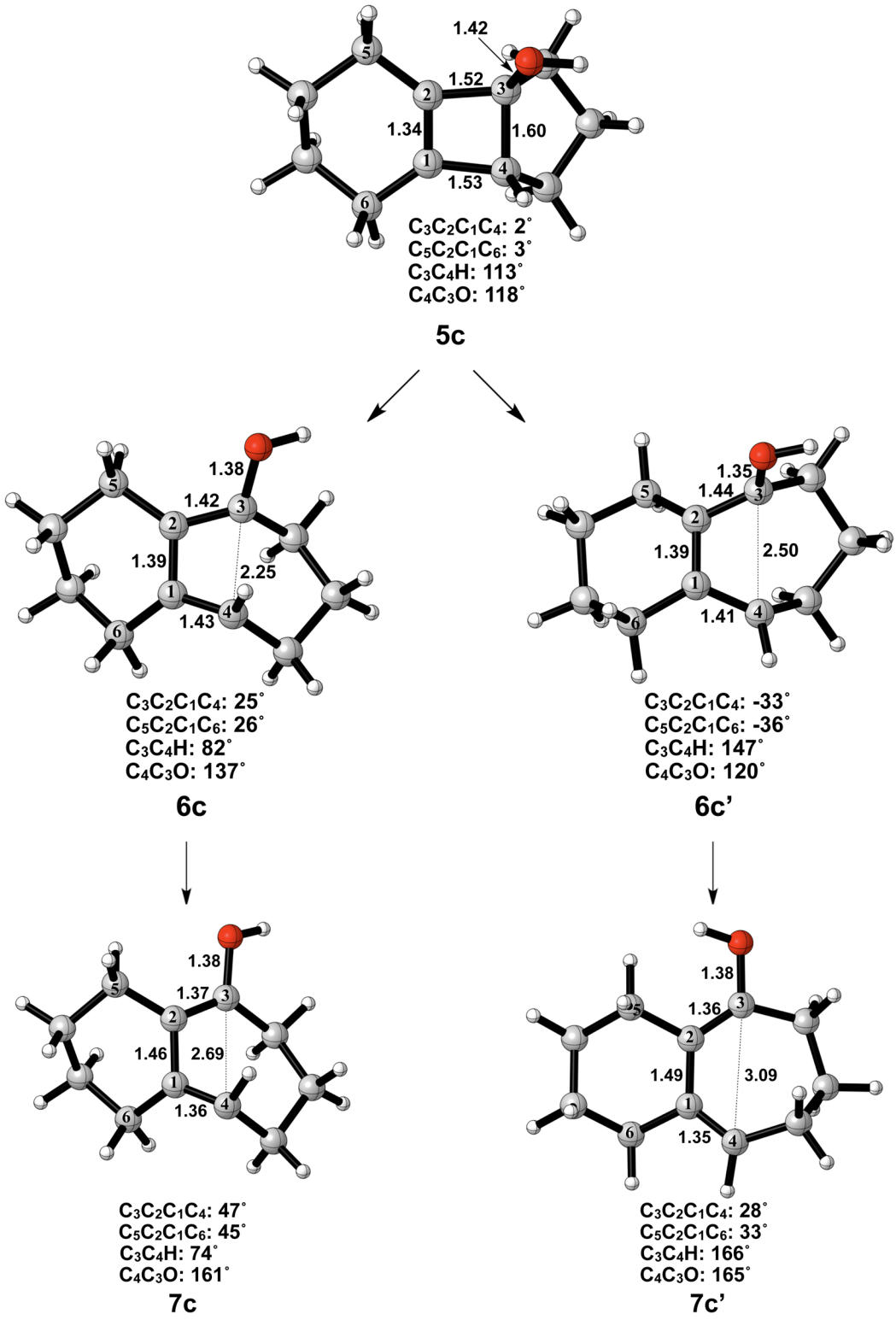

Figure 12.

Optimized geometries of conrotatory (left) and disrotatory (right) ring opening of cyclobutene alcohol **5c**. B3LYP/6-31G(d) selected bond distances (Å), angles, and dihedral angles are shown.

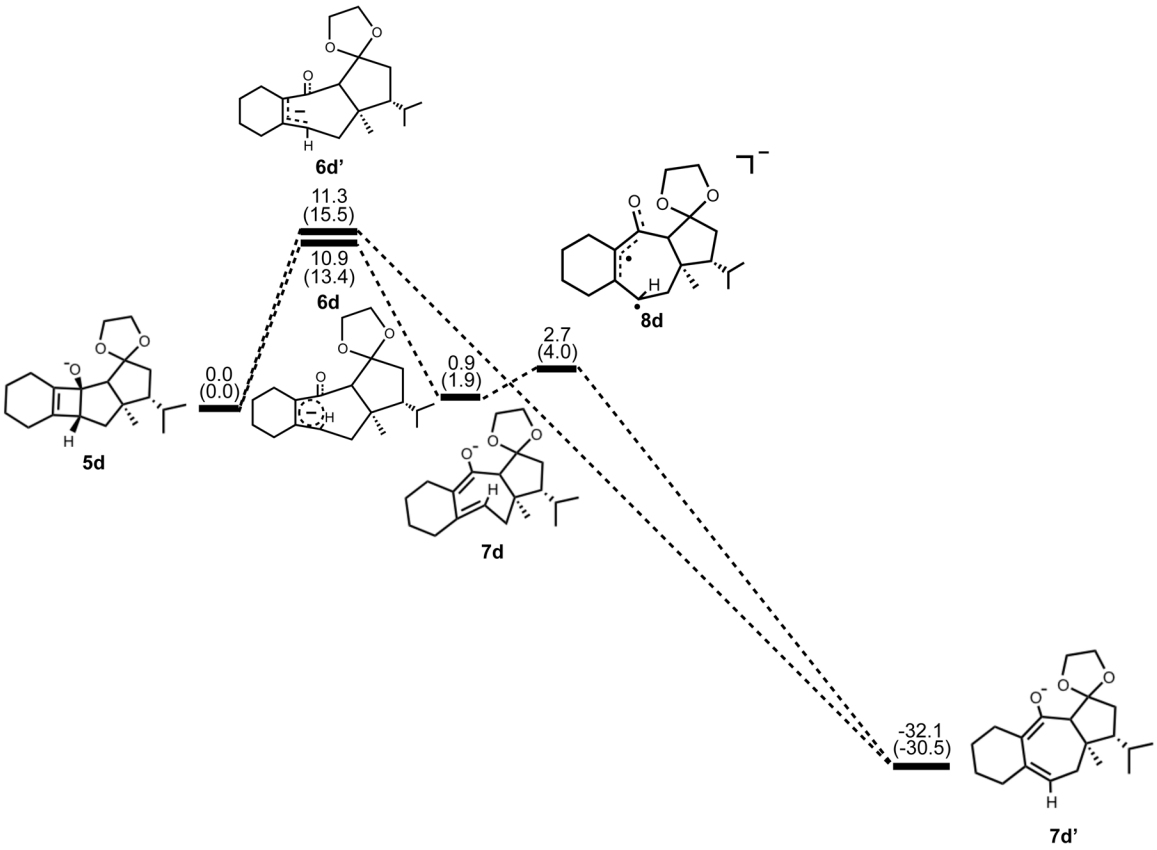

Figure 13.

Stationary points on the energy surface for electrocyclic ring opening of **5d**. B3LYP/6-31G(d) thermal energies, ΔH, with thermally corrected M06-2X/6-311++G(d,p)//B3LYP/6-31G(d) energies, ΔH, in parentheses, shown in kcal/mol.

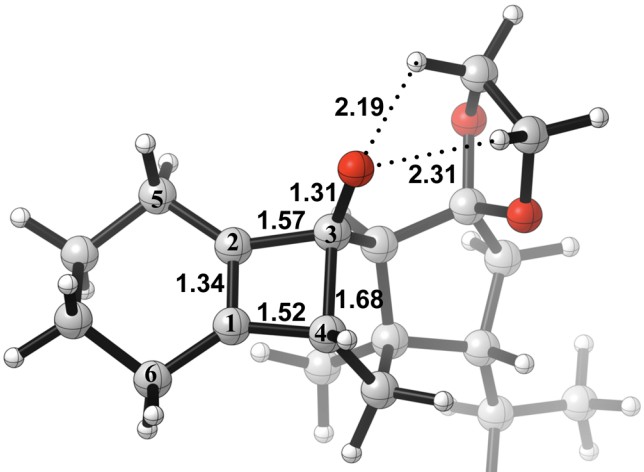

$C_3C_2C_1C_4$: 2° C_3C_4H: 112°
$C_5C_2C_1C_6$: -1° C_4C_3O: 122°

5d

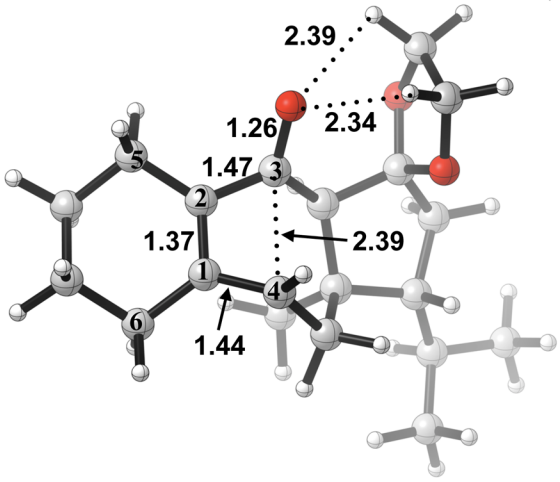

$C_3C_2C_1C_4$: -17° C_3C_4H: 94°
$C_5C_2C_1C_6$: -24° C_4C_3O: 137°

6d

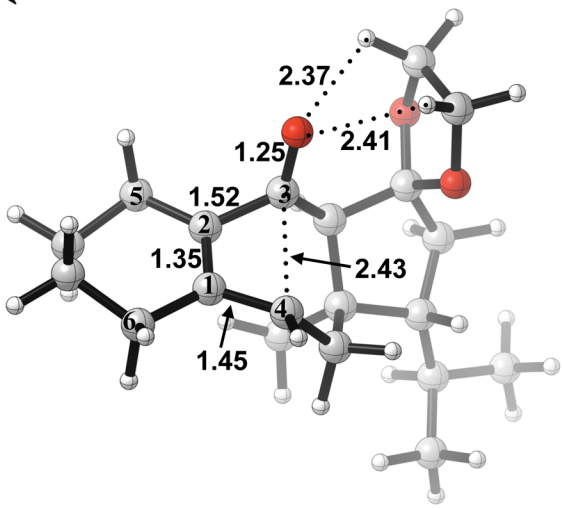

$C_3C_2C_1C_4$: 13° C_3C_4H: 141°
$C_5C_2C_1C_6$: 11° C_4C_3O: 121°

6d'

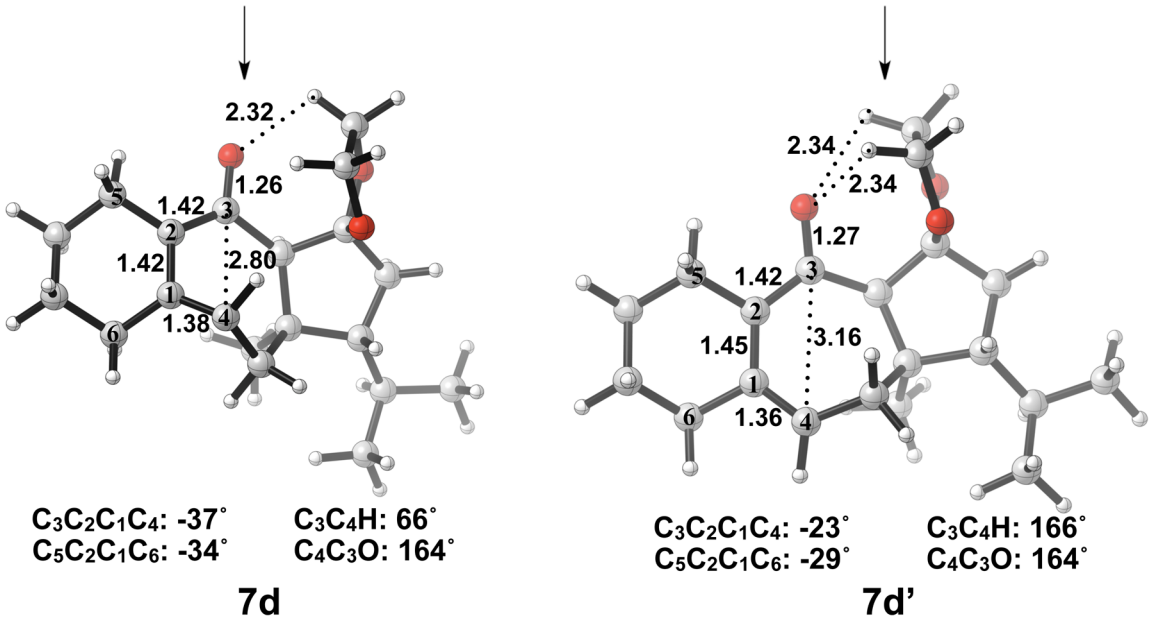

Figure 14.

Optimized geometries of conrotatory (left) and non-pericyclic (right) ring opening of **5d**. B3LYP/6-31G(d) selected bond distances (Å), angles, and dihedral angles are shown.

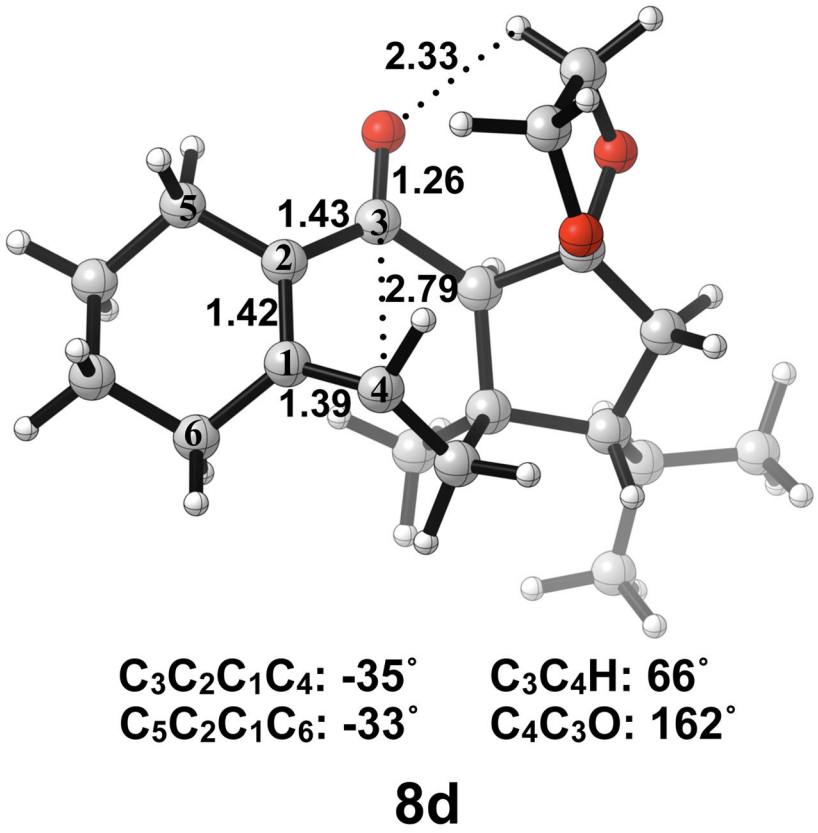

Figure 15.
Optimized transition structure of isomerization of alkoxide intermediate **7d** to **7d′**. B3LYP/6-31G(d) selected bond distances (Å), angles, and dihedral angles are shown.

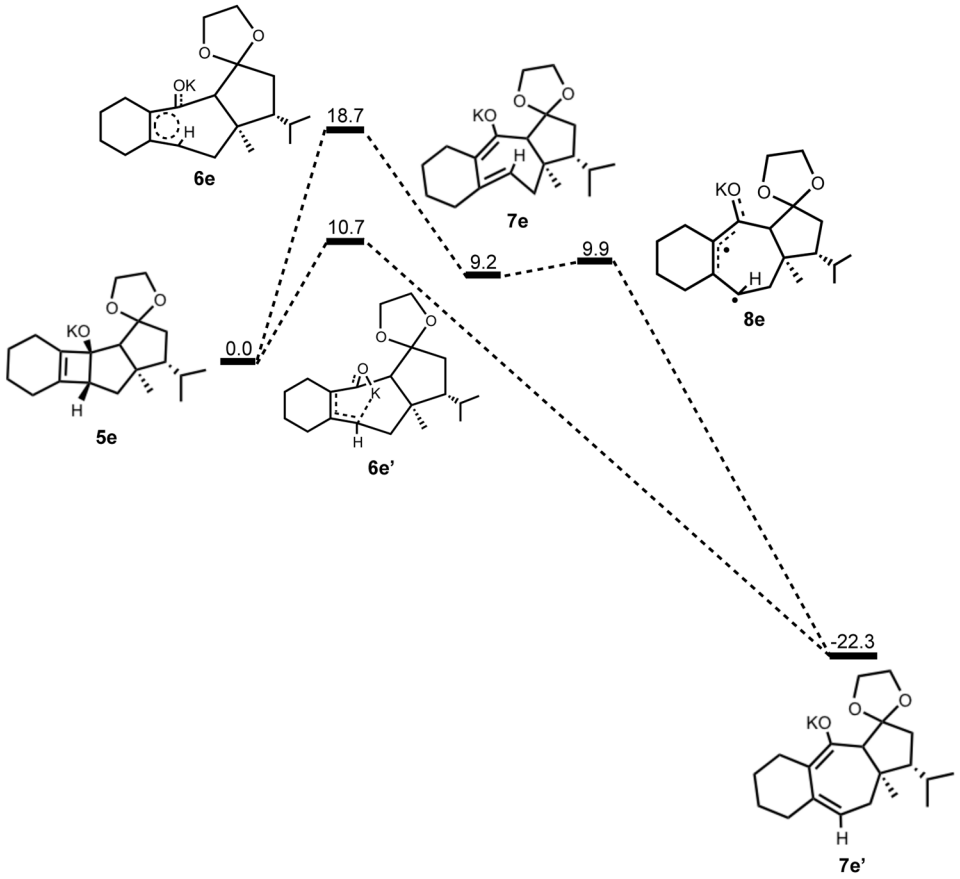

Figure 16.
Stationary points on the energy surface for electrocyclic ring opening of **5e**. B3LYP/6-31G(d) thermal energies, ΔH, shown in kcal/mol.

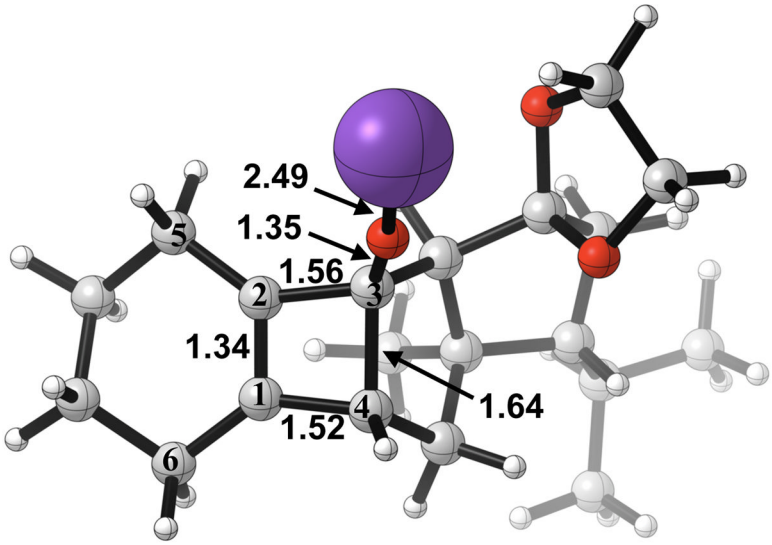

$C_3C_2C_1C_4$: 2° C_3C_4H: 114°
$C_5C_2C_1C_6$: 0° C_4C_3O: 121°

5e

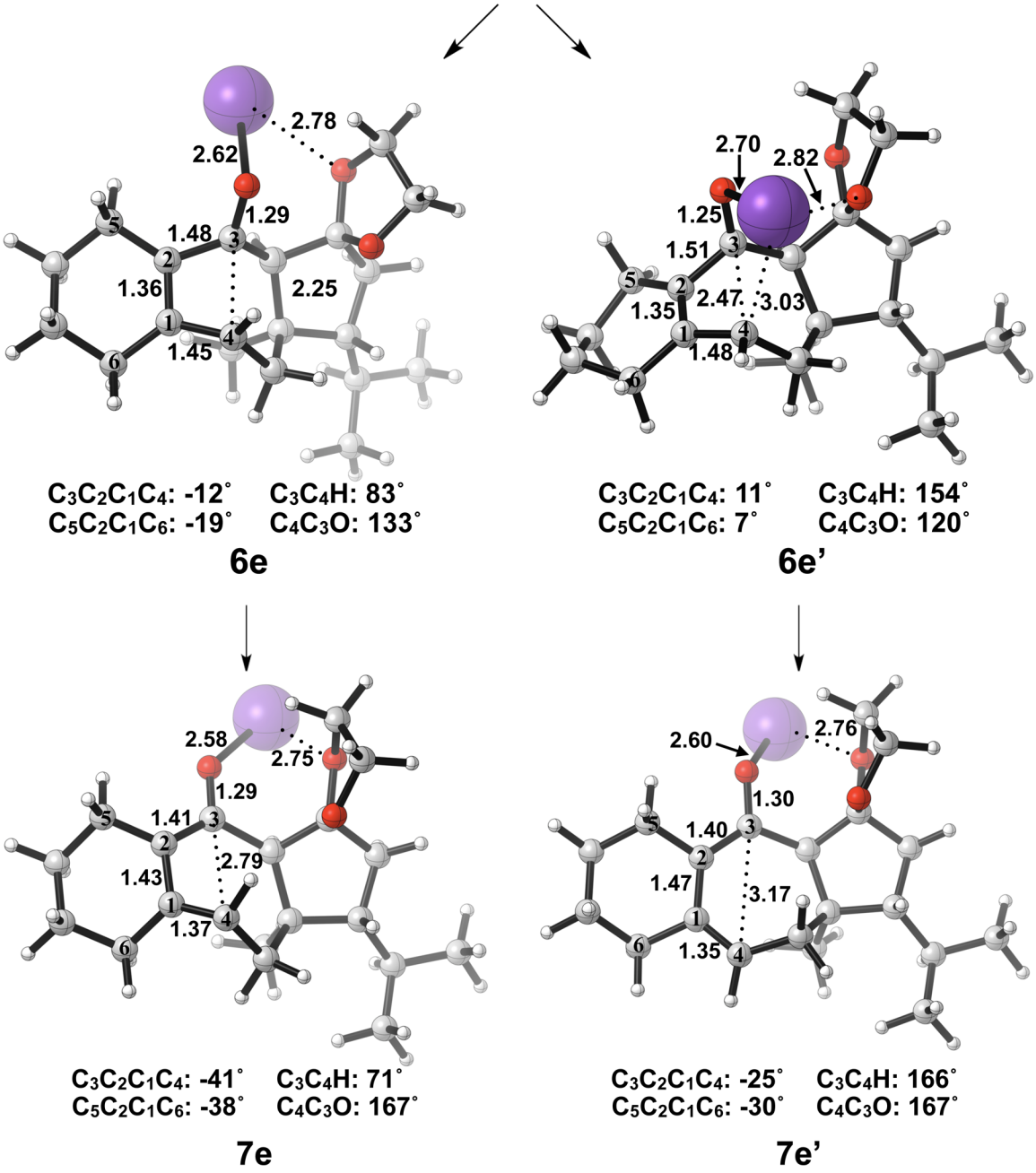

Figure 17.
Optimized geometries of conrotatory (left) and non-pericyclic (right) ring opening of **5e**. B3LYP/6-31G(d) selected bond distances (Å), angles, and dihedral angles are shown.

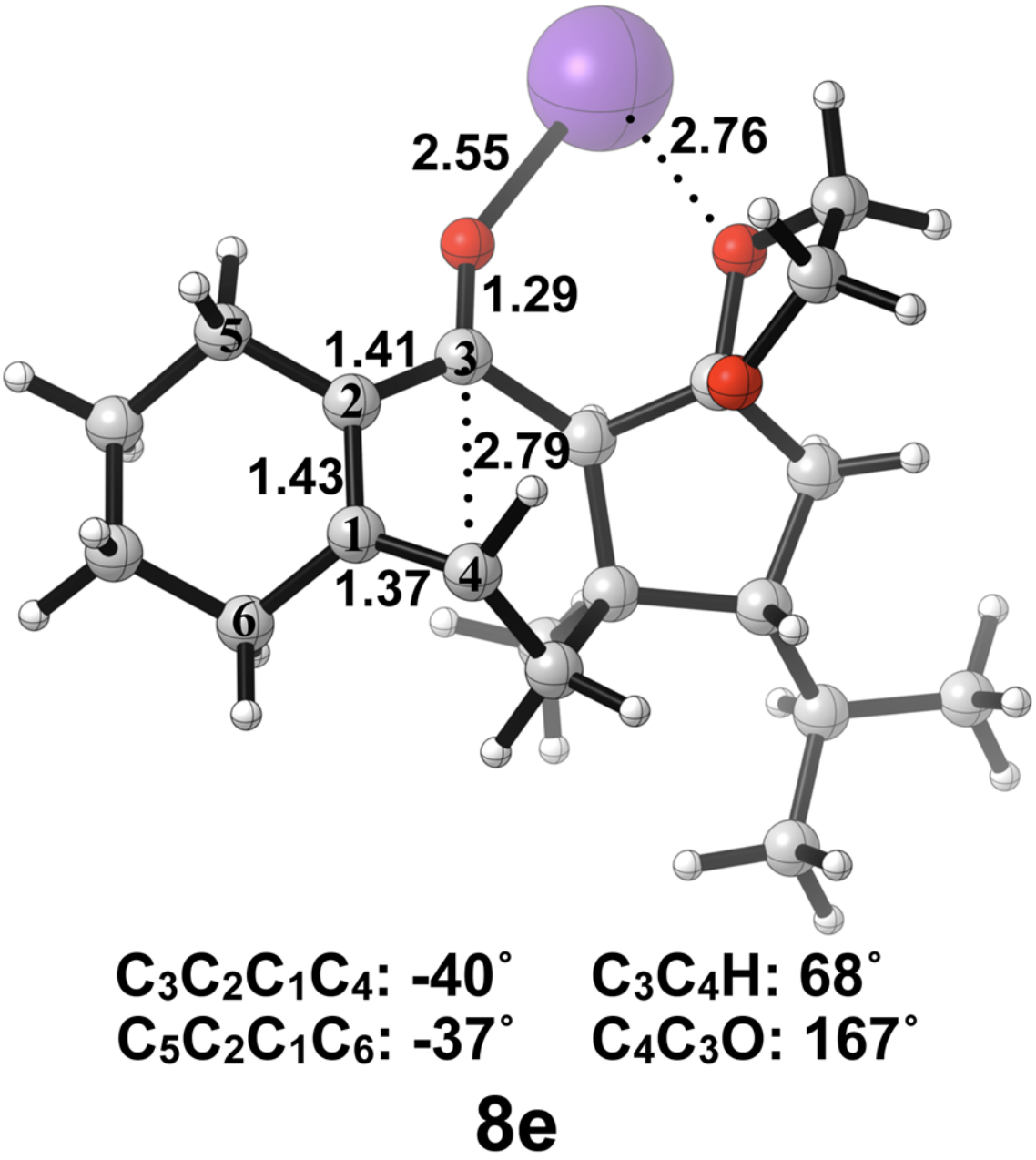

Figure 18.
Optimized transition structure of isomerization of potassium alkoxide intermediate **7e** to **7e′**. B3LYP/6-31G(d) selected bond distances (Å), angles, and dihedral angles are shown.

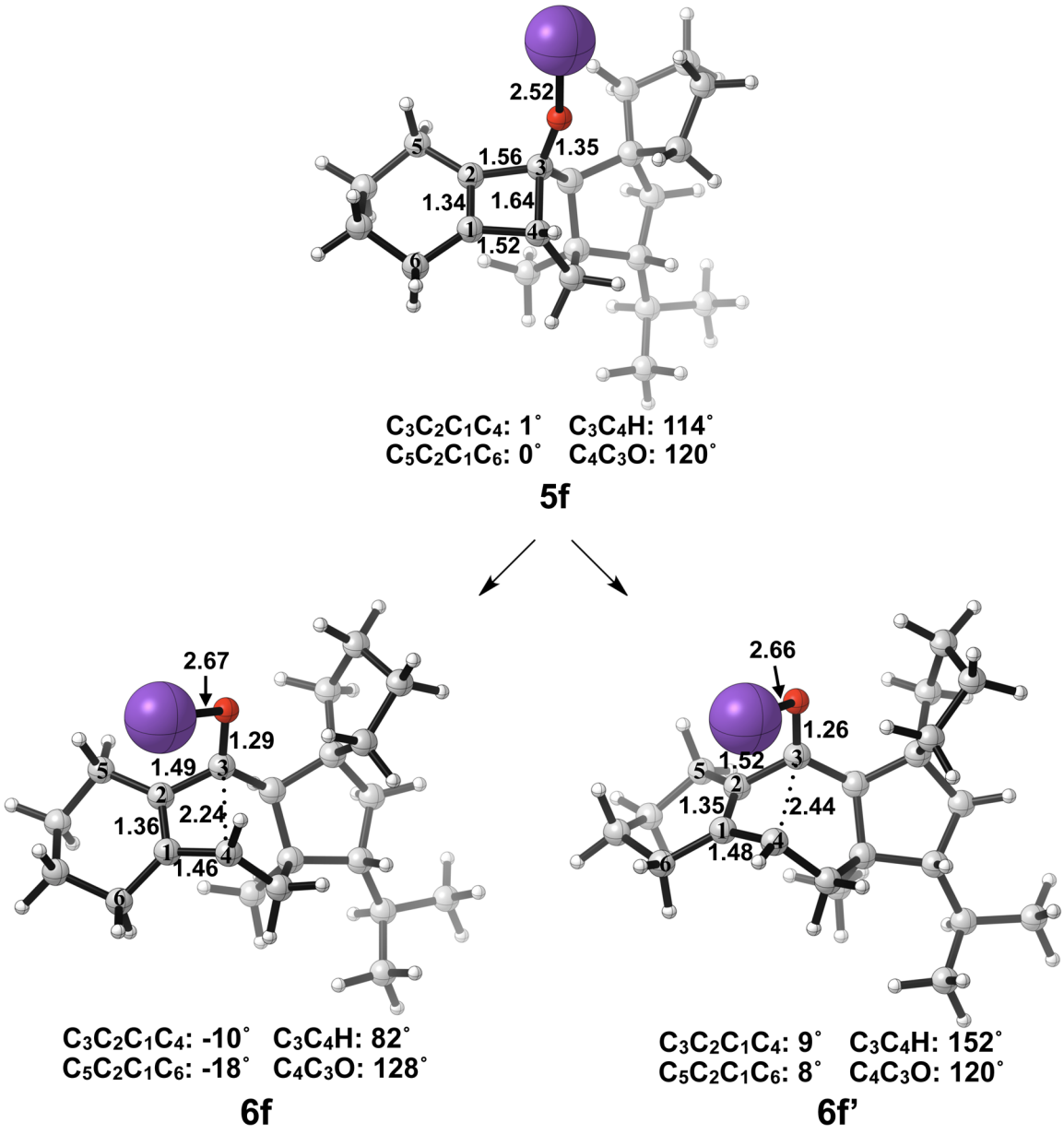

Figure 19.
Optimized geometries of conrotatory (left) and non-pericyclic (right) ring opening of **5f**. B3LYP/6-31G(d) selected bond distances (Å), angles, and dihedral angles are shown.

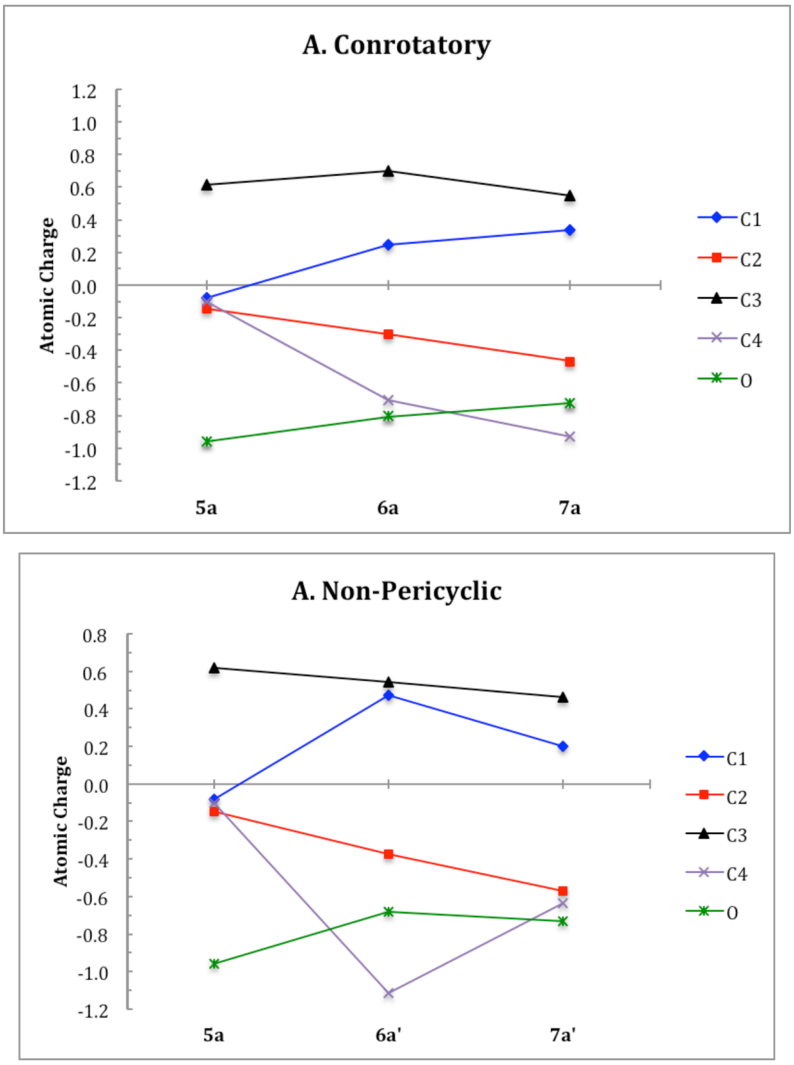

Figure 20.
Atomic charges on the four carbons and the oxygen substituent in the cyclobutene ring of **5a** throughout the two ring opening pathways.

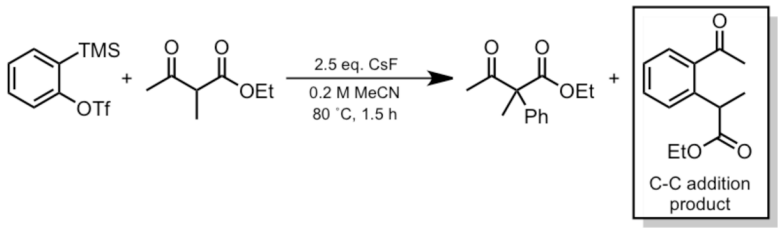

Scheme 1.
Acyl-Alkylation of Benzyne into a β-ketoester

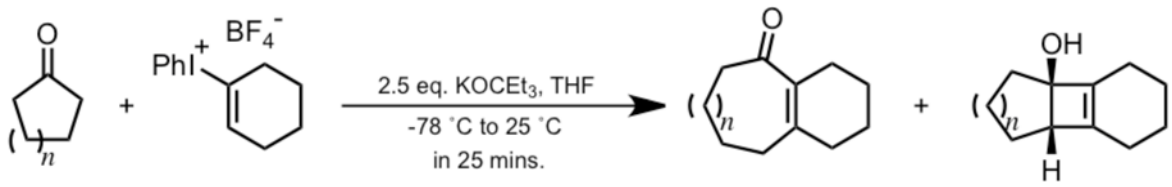

Scheme 2.
Cycloinsertion Reaction of Cyclohexyne into Cyclic Ketones

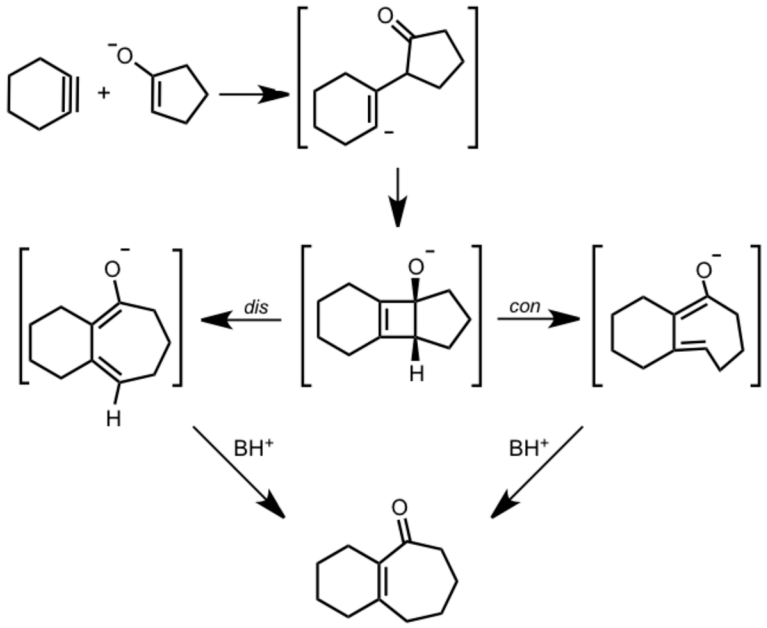

Scheme 3.
Proposed Mechanism of Cycloinsertion Reaction

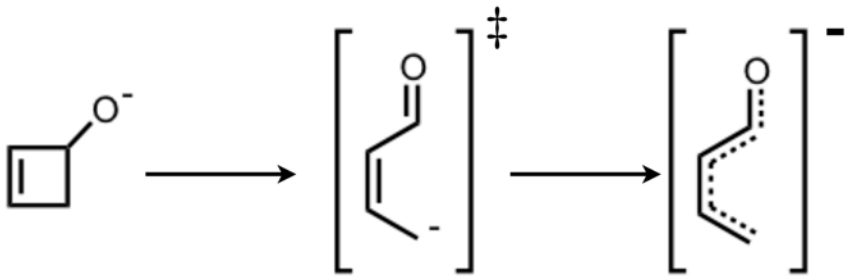

Scheme 4.
Schematic Representation of Non-Pericyclic Ring Opening

Table 1

Summary of computed enthalpies, ΔH, for the model alkoxide, potassium alkoxide, and alcohol systems.

	Gas Phase				THF		
	a			c	a		b
	B3LYP/6-31G(d)	B3LYP/6-311++G(d,p)	M06-2X	B3LYP/6-31G(d)	B3LYP/6-31G(d)	B3LYP/6-311++G(d,p)	B3LYP/6-31G(d)
1 + 2	0.0	0.0	0.0	-	0.0	-	0.0
3	−43.6	−35.9	−46.2	-	−33.8	-	−39.9
4	−41.8	−34.2	−41.3	-	−31.2	-	−36.9
5	−48.0	−41.6	−52.6	0.0	−41.5	0.0	−48.3
6	−45.5	−36.8	−46.6	28.3	−36.9	14.4	−33.7
6′	−44.4	−36.1	−43.8	47.5	−35.9	16.2	−33.0
7	−58.4	−49.6	−51.5	16.8	−48.5	3.1	−40.6
7′	−85.7	−75.3	−85.7	−13.9	−75.5	−22.5	−72.5
8	−44.0	−37.8	−47.7	−	-	-	−26.5

Table 2

Summary of computed enthalpies, ΔH, for the more complex alkoxide and potassium alkoxide guanacastepene precursors.

	Gas Phase		THF	
	d		e	f
	B3LYP/6-31G(d)	M06-2X	B3LYP/6-31G(d)	B3LYP/6-31G(d)
5	0.0	0.0	0.0	0.0
6	10.9	13.4	18.7	17.4
6′	11.3	15.5	10.7	13.7
7	0.9	1.9	9.2	-
7′	−32.1	−30.5	−22.3	-
8	2.7	4.0	9.9	-